



## Validation of a manufacturing process of pellets for bone filling and drug delivery

Emilie Chevalier, Marylène Viana, Sophie Cazalbou, Dominique Chulia

### ► To cite this version:

Emilie Chevalier, Marylène Viana, Sophie Cazalbou, Dominique Chulia. Validation of a manufacturing process of pellets for bone filling and drug delivery. *Journal of Drug Delivery Science and Technology*, 2008, 18 (6), pp.438-444. hal-03477035

**HAL Id: hal-03477035**

**<https://hal.science/hal-03477035>**

Submitted on 13 Dec 2021

**HAL** is a multi-disciplinary open access archive for the deposit and dissemination of scientific research documents, whether they are published or not. The documents may come from teaching and research institutions in France or abroad, or from public or private research centers.

L'archive ouverte pluridisciplinaire **HAL**, est destinée au dépôt et à la diffusion de documents scientifiques de niveau recherche, publiés ou non, émanant des établissements d'enseignement et de recherche français ou étrangers, des laboratoires publics ou privés.



## Open Archive TOULOUSE Archive Ouverte (OATAO)

OATAO is an open access repository that collects the work of Toulouse researchers and makes it freely available over the web where possible.

This is an author-deposited version published in : <http://oatao.univ-toulouse.fr/Eprints ID : 4825>

**To cite this version :** Chevalier, E. and Viana, Marylène and Cazalbou, Sophie and Chulia, Dominique (2008) *Validation of a manufacturing process of pellets for bone filling and drug delivery*. Journal of Drug Delivery Science and Technology, vol. 18 (n° 6). pp. 438-444. ISSN 1773-2247

Any correspondence concerning this service should be sent to the repository administrator: [staff-oatao@inp-toulouse.fr](mailto:staff-oatao@inp-toulouse.fr).

# Validation of a manufacturing process of pellets for bone filling and drug delivery

E. Chevalier<sup>1</sup>, M. Viana<sup>1\*</sup>, S. Cazalbou<sup>2</sup>, D. Chulia<sup>1</sup>

<sup>1</sup>Université de Limoges, CNRS SPCTS UMR 6638, Faculté de Pharmacie, Laboratoire de Pharmacie galénique,  
2, rue du Docteur-Marcland, 87025 Limoges Cedex, France

<sup>2</sup>CNRS CIRIMAT UMR 5085, Faculté des Sciences pharmaceutiques, Laboratoire de Pharmacie galénique,  
35, chemin des Maraîchers, 31062 Toulouse Cedex 09, France

\*Correspondence: marylene.viana@unilim.fr

*Wet high shear granulation followed by heat treatment was used to manufacture calcium phosphate porous spherical pellets. Experimental conditions were determined in order to obtain pellets presenting required specifications, i.e. size of about 800  $\mu\text{m}$ , maximum sphericity and high microporosity. These pellets were intended for bone defect filling and in situ drug delivery and the final step therefore consisted in ibuprofen loading. In a context of quality assurance, the aim of the present work was to validate each step of the manufacturing process (i.e. granulation, calcination and drug loading). Indeed, reproducibility of the pellet characteristics, especially the drug content and release kinetics from the ceramic to be implanted, has to be ensured through the manufacture quality control.*

**Key words:** High shear granulation – Heat treatment – Drug loading – Reproducibility – Process validation – Porous pellets – Drug delivery – Bioceramics.

Calcium phosphate ceramics are widely used as bone-graft materials [1-3] due to their chemical composition and crystalline structure similar to the mineral bone phase. These biomaterials are biocompatible, bioactive and osteoconductive [4-6]. To be effective for bone ingrowth, calcium phosphate bioceramics have to comply with certain specifications. In particular, macropore diameters must be at least 100  $\mu\text{m}$  to host the cellular and extracellular components of bone and blood vessels and greater than 200  $\mu\text{m}$  in diameter to allow osteoconduction [7]. Compared to the various physical presentations that are developed, calcium phosphate pellets present several advantages: they enable complex shaped bone defects to be filled while maintaining regular intergranular porosity due to their spherical shape.

High shear wet granulation may produce large granules, up to 1,000  $\mu\text{m}$ , from primary particles [8] and improve their flow properties [9]. This granulation consists in several steps: dry mixing in order to homogenize the initial powder mix, then wetting in order to induce nucleation and particle growth. The resulting agglomerates are finally dried. If spheronization, i.e. high speed rotation of the impeller without liquid addition, follows the agglomeration step, it is possible to manufacture spherical pellets.

In the context of a bone substitute development, the creation of intrapellet micropores is sought to promote chemical exchanges with the biological fluids and enhance bioactivity. As wet granulation binders are organic components, further heat treatment can remove them, thus creating intrapellet porosity. This additional microporosity can also be used to load pellets with therapeutic agents. The objective is to control the in situ release of the active pharmaceutical ingredient.

In as far as the implantation of biomaterials might be responsible for local inflammation [10-12], a novel therapeutic approach consists in the use of anti-inflammatory local delivery systems improving the bioavailability [10]. Among the anti-inflammatory agents suitable for drug delivery systems, ibuprofen was chosen as a model molecule since it is well documented and widely used [13].

One manufacturing process of porous spherical pellets involving high shear wet granulation followed by heat treatment was previously developed [14]. In the present paper, the aim is to validate the process in order to control, from one step to another, the properties of the final pellets. In fact, whatever the scale and field, reproducibility requirements

are of major importance to ensure constant end-use properties of the final product, i.e. for biomaterial application, morphology, textural properties, drug content of the pellets as well as release kinetics of the included drug substance.

This work describes each step of the manufacturing process of porous spherical phosphocalcic pellets loaded with ibuprofen. Four granulations are performed with the same process parameters and the corresponding batches are calcined and divided into three parts to be loaded. All along the process, the properties of four pellet batches are determined and compared in order to validate the manufacturing process and to evaluate its ability to produce pellets with the expected specifications concerning shape, size and porosity, as well as release characteristics.

## I. MATERIALS AND METHODS

### 1. Materials

A calcium phosphate derivative (CaP, batch number G8138/3, Cooper, France), consisting of two phases (monetite and hydroxyapatite) with a global Ca/P molar ratio equal to 1.5, was used as a pellet skeleton [14]. Pregelatinized starch (Sepistab ST 200, batch number 80551, Seppic, France) was used both as a binder for granulation and as a pore forming agent after elimination by heating. Ibuprofen (Ibuprofen 50, batch number IB1M738, BASF, Ludwigshafen, Germany) was used as drug substance.

### 2. Methods

#### 2.1. Pellet manufacturing process

Wet granulation process (*Figure 1*) was performed on 200 g of powder mix containing 10% of ST 200 in a Mi-Pro high shear granulator (Pro-C-epT, Zelzate, Belgium) equipped with a 1,900-mL capacity glass bowl, a three-blade impeller and a chopper.

In order to obtain the expected pellet characteristics (good sphericity, mean diameter around 800  $\mu\text{m}$  for macropore size of about 150  $\mu\text{m}$  and high microporosity) the following experimental conditions were applied [14-15]:

- mixing of the CaP and ST 200 powders at impeller and chopper speeds of 500 rpm for 180 s;
- granulation of the powder mix by addition of water at a distri-

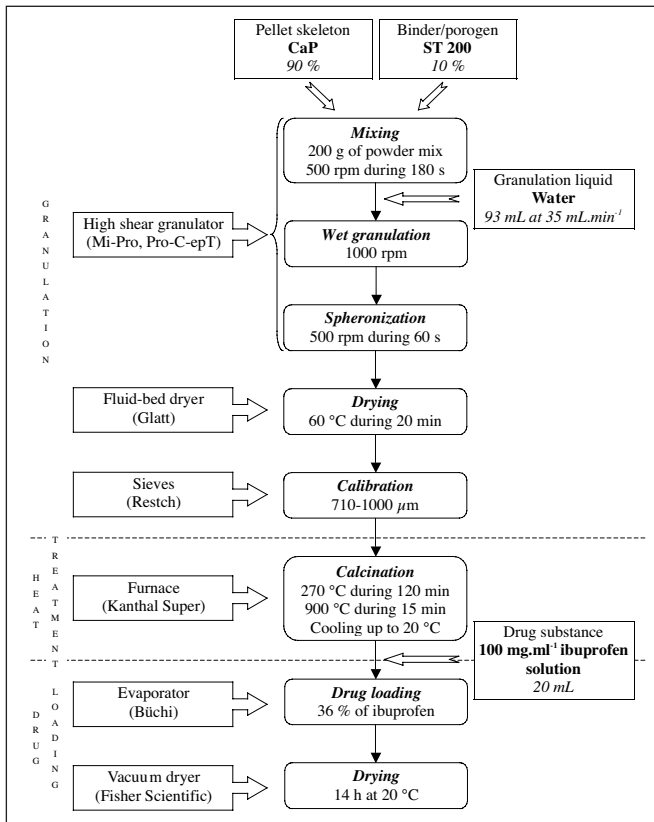


Figure 1 - Pellet elaboration chart.

bution rate of 35 mL.min<sup>-1</sup>, with impeller and chopper speeds of 1,000 rpm;  
- spheronization of the granules at impeller and chopper speeds of 500 rpm for 60 s.

Pellets thus obtained were dried in a fluidized bed (Glatt, Haltin-gen-Binzen/Baden, Germany) at 60°C for 20 min and finally sieved in order to retain the 710-1,000 μm fraction.

These granules were then submitted to a heat treatment, i.e. calcination (Kanthal Super, Rapid High Temperature Furnace, Bulten-Kanthal, Sweden) in order to remove the binder, thus acting as a pore former, and create the porosity. Pellets were first heated at 270°C with a heating rate of 2°C.min<sup>-1</sup> and maintained at this temperature for 2 h in order to burn out the pregelatinized starch. Then, in a second step, they were heated at the same heating rate, up to 900°C in order to obtain a monophasic component, β-TCP. This temperature was kept constant for 15 min before being cooling down at the rate of 10°C.min<sup>-1</sup> [14].

In order to validate the manufacturing process, four pellet batches were produced. Calcined pellets were then loaded with ibuprofen. In order to validate this step, 3.5 g of calcined pellets were sampled three times in each batch and loaded according to the following process: 20 mL of an ibuprofen ethanolic solution (100 mg.mL<sup>-1</sup>) were introduced in a 250 mL flask containing the pellets and were evaporated in a Rotavapor (Büchi, Switzerland). Then, pellets were vacuum-dried at 20°C in an oven (model 45001, Fisher Bioblock Scientific, Illkirch, France) for 14 h. The theoretical ibuprofen ratio in the loaded pellets was equal to 36%.

## 2.2. Raw material and unloaded pellet physicochemical characterizations

### 2.2.1. Particle size

The raw material size distribution was determined in triplicate with a laser diffraction analyzer (Mastersizer 2000, Malvern Instruments Ltd, Worcestershire, UK) under dry conditions. The median diameter ( $d_{0.5}$ , μm) was determined from the distribution curve.

### 2.2.2. Pycnometric density

Pycnometric density ( $d_{\text{pycno}}$ , g.cm<sup>-3</sup>) was determined using a helium pycnometer AccuPyc 1330 (Micromeritics Instruments Inc., Norcross, GA, USA). Prior to measurements, samples were degassed at a pressure lower than 50 mTorr vacuum (VacPrep 061, Micromeritics Instruments Inc., Norcross, GA, USA). Measures were repeated until the value stabilized [16].

### 2.2.3. Specific surface area

Specific surface area ( $S_{\text{spe}}$ , m<sup>2</sup>.g<sup>-1</sup>) was measured by nitrogen ad-sorption using a Gemini 2360 Analyzer (Micromeritics Instruments Inc., Norcross, GA, USA). Measurements were repeated until the value stabilized. Prior to evaluation, samples were degassed under the same conditions as for pycnometric density measurements. The specific surface areas were calculated from the BET multipoint equation [17] in the relative range of pressure of 0.05-0.30. In all cases, sample quantities ensured a total measured surface of at least 1 m<sup>2</sup>.

### 2.2.4. Morphology

Raw material morphology and texture were observed using scanning electron microscopy (SEM, Stereoscan S260, Leica, Cambridge, UK).

Granule morphology was observed by optical microscopy (MZ 16, Leica, Cambridge, UK). The pellet sphericity was determined by calculating the circularity coefficient on 20 pellets per batch with the Image J free software [18]. The circularity formula is the following:

$$\text{Circularity} = 2 \sqrt{\pi \times \text{area}} / \text{perimeter} \quad \text{Eq. 1}$$

### 2.2.5. Porosity

Porosity measurements were carried out with a mercury intrusion porosimeter (Autopore IV 9500, Micromeritics Instruments Inc., Norcross, GA, USA) with a 5-cm<sup>3</sup> powder penetrometer. Cumulative and differential intrusion curves were recorded. The intrusion volume  $V_{\text{intra}}$  (mL.g<sup>-1</sup>) corresponding to the pellet porosity was deduced and the corresponding pore size diameters were noted.

The pellet porosity (%) was calculated according to Equation 2:

$$\text{Pellet porosity (\%)} = [V_{\text{intra}} / (V_{\text{solid}} + V_{\text{intra}})] \times 100 \quad \text{Eq. 2}$$

where  $V_{\text{solid}}$ , the volume occupied by the solid fraction of the granules, was determined by pycnometric measurements.

The inter-pellet porous volume  $V_{\text{inter}}$  (mL.g<sup>-1</sup>) was calculated according to:

$$V_{\text{inter}} \text{ (mL.g}^{-1}\text{)} = V_{\text{packed}} - V_{\text{pellets}} = V_{\text{packed}} - (V_{\text{intra}} + V_{\text{solid}}) \quad \text{Eq. 3}$$

where  $V_{\text{packed}}$  (mL.g<sup>-1</sup>) was the apparent volume obtained by close packing of pellets without any agglomerate deformation [19] and  $V_{\text{pellets}}$  (mL.g<sup>-1</sup>) was the volume of the pellets.

The pellet bed which would result from the organization of unloaded pellets inside the bone defects could be characterized by the inter pellet porosity, i.e. macroporosity of the bone filling material according to:

$$\text{Macroporosity (\%)} = (V_{\text{inter}} / V_{\text{packed}}) \times 100 \quad \text{Eq. 4}$$

The total porosity of the biomaterial such elaborated, composed of both macroporosity and microporosity, therefore equalled:

$$\text{Total porosity (\%)} = [(V_{\text{inter}} + V_{\text{intra}}) / V_{\text{packed}}] \times 100 \quad \text{Eq. 5}$$

## 2.3. Dissolution kinetics

*In vitro* release studies were performed on about 550 mg of loaded pellets in 500 mL of phosphate buffer solution (pH 7.48) at 37°C using

an USP II apparatus (Prolabo Dissolution Tester, France) equipped with a paddle stirrer rotating at 100 rpm. Three millilitres of dissolution medium were withdrawn at regular intervals up to 300 min and the quantity of ibuprofen was determined by UV absorption spectrophotometry at 264 nm. The volume reduction of the dissolution medium was taken into account to calculate the concentration values. The dissolution test was performed in triplicate, 36 samples were thus analyzed, corresponding to the three loaded fractions of the four pellet batches.

The dissolution profiles were established as the cumulative percentage of drug released (Q, %) related to the theoretical ibuprofen quantity, i.e. 200 mg versus the time (T, min). As a comparison, dissolution kinetics were also determined, in triplicate, on a CaP/ibuprofen mix containing 36% of ibuprofen.

In order to validate each step of the manufacturing process, dissolution kinetics were analyzed according to the following methodology (Figure 2):

- first level: the homogeneity of the drug loading and release was studied by calculating the coefficient of variation (CV) in each time point of the triplicate dissolution profiles (1, 2, 3) for each loaded part (A, B, C). The area under curve (AUC) was calculated at t = 300 min for each kinetics, using the Weibull function [20], and the coefficient of variation of the triplicate was expressed;
- second level: in order to validate the drug loading reproducibility, the CV of the nine AUC values, determined from the dissolution profiles of each pellet batch, was calculated;
- third level: CV of the AUC calculated from the 36 kinetics was determined in order to validate the whole manufacturing process. The inter- and intra-batch drug content variability was studied using an analysis of variance model II [21, 22], allowing a non-biased estimation of drug content variability. Variances were compared between the four batches using a two-sided Fisher test. This test can be applied since the environmental conditions were maintained constant during the manufacture of the four batches.

In order to determine the release mechanism, dissolution data were then fitted to the Higuchi [23], Hixson-Crowell [24], Ritger and Peppas [25] and Kopcha [26] models.

II. RESULTS AND DISCUSSION  
1. Raw material characterization

Raw material characteristics are listed in Table I. SEM analyses showed small acicular CaP particles as compared with ST 200, composed of large agglomerates of elementary starch particles (around 10 μm). Ibuprofen presented elongated particles. Pycnometric density of CaP confirmed the presence of the two phases (monetite and hydroxyapatite) in so far as the value measured was lower than the

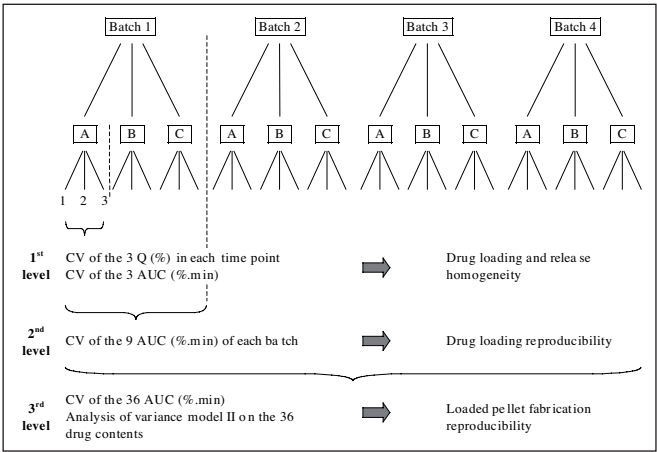


Figure 2 - Chart for the manufacturing process validation.

theoretical β-TCP density (2.95 versus 3.07 g.cm<sup>-3</sup>) [14]. The specific surface area of CaP was particularly high, compared to the ST 200 value, in accordance with the small particle size. Ibuprofen specific surface area was measured by nitrogen adsorption but was too low (< 0.20 m<sup>2</sup>.g<sup>-1</sup>) to be precisely determined.

2. Unloaded pellet characteristics

The results of the physicochemical characterizations performed on the four batches of the unloaded pellets, respectively before and after heat treatment, are listed in Table II. Incremental mercury intrusion curves are plotted on Figure 3.

For uncalcined pellets, the variation coefficients lower than 3%, whatever the considered parameter, clearly indicated the similarity of the four batches, thus confirming the reproducibility of the granulation process.

Pycnometric density values highlighted the homogeneous composition of the pellets as the theoretical density value, calculated from the theoretical composition of the pellets, equaled 2.70 g.cm<sup>-3</sup>.

Uncalcined pellets exhibited a high specific surface area (33.35 m<sup>2</sup>.g<sup>-1</sup>). This value slightly decreased compared to that of the CaP major component of the pellets (36.50 m<sup>2</sup>.g<sup>-1</sup>), due to the granulation with 10% of ST 200, presenting a very low specific surface area.

Circularity coefficient was 0.83, indicating the ability of the high shear granulation followed by the spheronization to produce relatively spherical pellets.

Porograms of the four pellet batches (Figure 3) were superimposed assuming the reproducibility of the porosity created during the granulation process. They displayed two main pore ranges for which

Table I - Raw material characteristics.

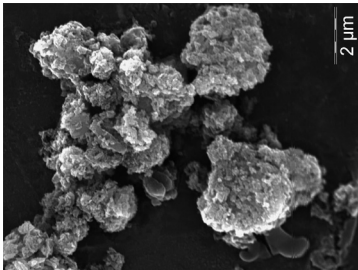
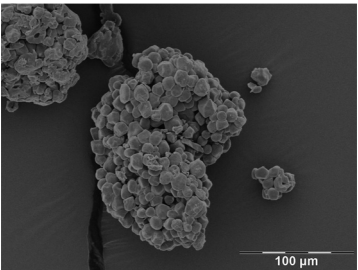
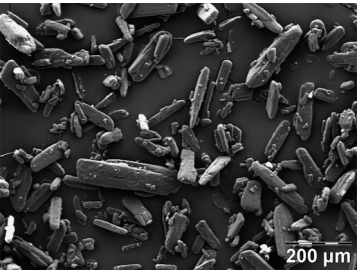
Materials	CaP	ST 200	Ibuprofen
Function	Pellet skeleton	Binder/pore former	Drug substance
Morphology			
d <sub>0.5</sub> (μm)	7	207	50
D <sub>pycno</sub> (g.cm <sup>-3</sup> )	2.95 ± 0.00	0.44 ± 0.00	1.11 ± 0.00
S <sub>spe</sub> (m <sup>2</sup> .g <sup>-1</sup> )	36.50 ± 0.68	1.50 ± 0.00	< 0.20



Table II - Unloaded pellet characteristics.

	Before heat treatment					After heat treatment				
	Batch 1	Batch 2	Batch 3	Batch 4	Mean value (CV%)	Batch 1	Batch 2	Batch 3	Batch 4	Mean value (CV%)
D <sub>pycno</sub> (g.cm <sup>-3</sup> )	2.70	2.71	2.70	2.70	2.70 (0.00)	3.04	3.04	3.04	3.05	3.04 (0.00)
S <sub>spe</sub> (m <sup>2</sup> .g <sup>-1</sup> )	32.78	33.20	33.45	33.96	33.35 (1.49)	5.67	5.64	5.78	5.67	5.69 (1.05)
Circularity coefficient	0.80	0.85	0.83	0.82	0.83 (2.52)	0.83	0.83	0.83	0.82	0.83 (0.60)
Pellet pore size diam. range (nm)	[6-150] [150-1000]	[6-150] [150-1000]	[6-150] [150-1000]	[6-150] [150-1000]	-	[90-400] [400-4000]	[90-400] [400-4000]	[90-400] [400-4000]	[90-400] [400-4000]	-
V <sub>intra</sub> (mL.g <sup>-1</sup> )	0.33	0.34	0.33	0.34	0.34 (2.94)	0.45	0.44	0.45	0.44	0.45 (2.22)
V <sub>solid</sub> (mL.g <sup>-1</sup> )	0.37	0.37	0.37	0.37	0.37 (0.00)	0.33	0.33	0.33	0.33	0.33 (0.00)
V <sub>packed</sub> (mL.g <sup>-1</sup> )	1.26	1.25	1.24	1.25	1.25 (0.80)	1.30	1.27	1.29	1.30	1.29 (0.78)
V <sub>inter</sub> (mL.g <sup>-1</sup> )	0.56	0.54	0.54	0.54	0.55 (1.82)	0.52	0.51	0.51	0.53	0.52 (1.92)
Pellet porosity (%)	47.1	47.9	47.1	47.9	47.5 (0.8)	57.7	57.1	57.7	57.1	57.4 (0.5)
Macroporosity (%)	44.4	43.2	43.5	43.2	43.6 (1.4)	40.0	39.8	39.5	40.8	40.1 (1.2)
Total porosity (%)	70.6	70.4	70.2	70.4	70.4 (0.3)	74.6	74.2	74.4	74.6	74.5 (0.3)

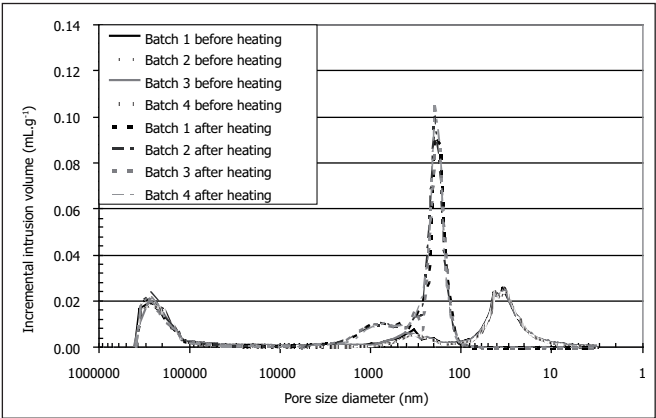


Figure 3 - Incremental porograms for pellets before and after calcination.

culated volumes are given in Table II. The first, which was located around 100 to 300  $\mu\text{m}$  for all batches, corresponded to the interpellet porosity. However, this porosity was under estimated due to the measurement range (lower than 300  $\mu\text{m}$ ) of the mercury porosimeter; its true value was thus calculated (Table II) from the packed ( $V_{\text{packed}}$ ) and the solid ( $V_{\text{solid}}$ ) volumes of the granules as previously described. The porosity was around 44% and corresponded to the macroporosity of the pellet bed. Macropores were higher than 100  $\mu\text{m}$  in diameter and could therefore host the cellular and extracellular components of bone and blood vessels and as a high proportion was greater than 200  $\mu\text{m}$  in size, they would be favorable to osteoconduction [7] in the case of implantation into bone defect cavities. The second intrusion range, around [6-150] nm and [150-1,000] nm corresponded to the intragranular porosity, called pellet porosity in this work, and was equal to 47.5% corresponding to 26% when related to the volume occupied

by the pellet bed. A total porosity of around 70% was thus estimated in the biomaterial and was composed of 44% of macropores and 26% of micropores.

Similarity between the different characteristics determined on the four calcined batches was also observed, as shown by coefficients of variation lower than 2.5%. The reproducibility of the thermal treatment effect was therefore demonstrated. However, the comparison of the characteristics before and after heat treatment clearly highlighted the influence of the calcination.

In fact, it induced the removal of the pore former [14] and chemical modifications by improving the crystallinity and the coalescence of the elementary particles [27]. After heating, the initial biphasic CaP became a monophasic  $\beta$ -TCP component and the measured pycnometric density was thus close to the theoretical value (3.07 g.cm<sup>-3</sup>).

Specific surface area dramatically decreased (5.69 m<sup>2</sup>.g<sup>-1</sup> versus 33.35 m<sup>2</sup>.g<sup>-1</sup>) despite porogen removal. Raynaud *et al.* [28] explained that the surface reduction during heat treatment was attributed to elementary particle coalescence without shrinkage, from superficial diffusion.

Circularity coefficient was unchanged after heat treatment and sphericity (0.83) was preserved.

As for uncalcined batches, porograms of the four calcined samples were superimposed and confirmed the reproducibility of the thermal treatment. Incremental intrusion curves presented two main steps. The interpellet porosity was composed of pores with a median diameter higher than 100  $\mu\text{m}$  and the corresponding macroporosity was around 40%. Pellet porosity consisted of two ranges of pore size [90-400] and [400-4,000] nm and was around 57.4%. This result highlighted a 10% increase in porosity as compared with the uncalcined pellet porosity (47.5% versus 57.4% after heat treatment). This phenomenon was due to the removal of ST 200 and the porosity increase was close to the initial amount of pore former.

**Table III** - Coefficient of variation (CV) in each time point of the dissolution profiles (%).

Time (min)	Batch											
	1			2			3			4		
	A	B	C	A	B	C	A	B	C	A	B	C
0	0.00	0.00	0.00	0.00	0.00	0.00	0.00	0.00	0.00	0.00	0.00	0.00
5	16.02	9.87	1.51	11.67	2.66	17.68	6.38	3.60	13.45	11.27	9.87	4.18
10	2.55	3.80	0.35	1.30	1.13	3.52	6.72	2.40	7.55	4.48	3.80	1.86
15	5.22	4.39	0.95	3.45	1.86	4.11	1.39	3.79	3.83	2.90	4.39	1.34
20	2.68	4.44	1.08	1.97	0.87	2.77	0.81	4.89	2.39	2.14	4.44	1.02
30	1.70	2.82	1.03	1.02	1.53	2.55	3.10	5.27	0.40	1.63	2.82	0.75
45	2.31	2.17	1.22	1.31	0.40	1.94	1.48	4.21	1.52	1.06	2.17	1.33
60	0.55	2.21	1.17	1.78	1.29	2.24	0.98	3.03	1.92	0.83	2.21	0.59
90	1.67	2.19	0.67	1.43	0.86	2.16	1.50	2.72	2.48	1.03	2.19	0.48
120	1.93	1.69	0.78	0.80	1.06	2.54	0.72	0.45	1.55	0.80	1.69	0.47
150	1.10	1.22	1.01	0.76	0.92	2.62	0.16	0.63	0.94	0.65	1.22	0.43
180	0.87	1.56	1.12	1.34	0.63	1.97	1.50	1.29	1.58	0.95	1.56	0.76
210	2.10	1.76	1.23	0.88	1.38	1.42	0.89	0.70	1.32	0.43	1.76	0.82
240	1.42	1.77	0.63	0.62	1.07	3.13	0.73	1.25	1.04	0.91	1.77	1.17
270	1.18	1.72	1.37	0.87	1.19	3.11	0.68	0.59	1.05	0.08	1.72	0.99
300	0.97	1.92	0.71	1.01	1.08	2.05	0.31	1.03	1.61	1.98	1.92	1.48

**Table IV** - Coefficient of variation of the AUC values.

Granulation	Load-ing	Re-release	AUC (%.min)	CV (%)		
Batch 1	A	1	443.10	1.0	2.0	2.9
		2	435.30			
		3	435.80			
	B	1	446.60	1.8		
		2	451.50			
		3	462.80			
	C	1	436.50	1.1		
		2	437.80			
		3	445.80			
Batch 2	A	1	445.80	0.9	2.4	
		2	453.10			
		3	446.90			
	B	1	442.50	0.8		
		2	437.80			
		3	445.20			
	C	1	420.00	2.2		
		2	438.40			
		3	426.60			
Batch 3	A	1	429.40	0.4	1.6	
		2	427.90			
		3	431.30			
	B	1	440.30	0.8		
		2	439.10			
		3	446.10			
	C	1	434.70	1.4		
		2	423.80			
		3	434.30			
Batch 4	A	1	416.30	0.8	4.2	
		2	413.90			
		3	420.50			
	B	1	426.30	5.2		
		2	471.90			
		3	459.10			
	C	1	441.70	0.6		
		2	447.00			
		3	443.50			

**Table V** - Drug content of the 36 loaded samples.

Granulation	Loading	Release	Drug content (mg)
Batch 1	A	1	200.60
		2	198.50
		3	201.90
	B	1	199.80
		2	200.80
		3	206.30
	C	1	199.50
		2	199.20
		3	204.80
Batch 2	A	1	204.40
		2	206.20
		3	203.60
	B	1	200.70
		2	199.20
		3	200.00
	C	1	193.30
		2	203.40
		3	200.40
Batch 3	A	1	197.80
		2	196.50
		3	195.80
	B	1	201.60
		2	198.00
		3	199.90
	C	1	198.60
		2	195.30
		3	198.90
Batch 4	A	1	194.60
		2	192.70
		3	196.30
	B	1	188.10
		2	206.30
		3	201.50
	C	1	202.00
		2	206.10
		3	201.90

3. Release kinetics

Coefficients of variation in each time point and AUC values of the 36 dissolution profiles are recapitulated in *Tables III and IV*, as well as the corresponding drug contents, deduced from the final released quantity, in *Table V*. They were discussed thereafter in order to validate the manufacturing process.

- First level: CV in each time point (*Table III*) of the triplicate dissolution profiles (1, 2, 3), calculated for each loaded part A, B, C (*Figure 2*), were around 5%, except for the first point 5 min (lower than 18%). For several authors [29-30], a CV ≤ 10% was required as a limit value, with an allowance up to 20% for the first experimental point, to consider mean dissolution data. Consequently, the calculated CV values highlighted the reproducibility of the release and the drug loading homogeneity. Moreover, as far as AUC values were determined for the same period of time (300 min), the CV values, lower than 5.5% (*Table IV*), confirmed the drug loading homogeneity and the release reproducibility. It should be noted that the previous observations also validated the dissolution test procedure.

- @Second level: AUC values calculated from the nine dissolution profiles of all loaded fractions (A, B, C) still presented a low coefficient of variation, less than 4.5% in this case (*Table IV*), thus suggesting reproducibility of the loading procedure and the release efficiency for each granulation batch.

- Third level: CV of the AUC values was low and even lower than those observed in the previous step (2.9% vs. 4.2%). This result, concerning the 36 samples, thus indicated that it did not exist a higher inter-batch variability than the intra-batch one (9 profiles). On the basis of the three previous conclusions concerning the CVs, all the dissolution profiles could be considered as similar. The drug content variability was then studied using the analysis of variance model II. This statistical test considered two sources of variation, inter and intrabatch variabilities, corresponding respectively to granulation and loading procedures. Variance values thus calculated indicated no statistical difference between the drug contents either due to the loading procedure (σ² = 1.81) or to the granulation step (σ² = 1.02), at a statistical risk (p value) of 5% (*Table V*). A comparison of the mean (199.8 ± 4.1 mg) with the theoretical ibuprofen content (200 mg) indicated that the difference was not significant, at a statistical risk of 5%. It clearly demonstrated that the whole expected quantity of ibuprofen was loaded into the pellets and entirely released.

As granulation, loading and release step reproducibility was validated, it was possible to consider only a mean dissolution profile of the 36 loaded samples (*Figure 4*). The comparison with the kinetics obtained from a reference CaP/ibuprofen mix highlighted a sustained release of ibuprofen. In fact, the whole quantity of ibuprofen was totally dissolved in 10 min from the powder mix whereas the total quantity was released after 240 min in the case of the loaded pellets. Thereafter, dissolution data were modeled in order to determine the release mechanism occurring during the dissolution. The correlation coefficients (r²) for Higuchi, Hixson-Crowell, Ritger-Peppas and Kopcha models as well as the characteristic parameters of Ritger-Peppas and Kopcha equations are given in *Table VI*. Dissolution data closely fitted both to Higuchi and Hixson-Crowell, and so either erosion or diffusion might be involved, but Ritger-Peppas n exponent (< 0.43) and Kopcha A/B ratio (> 1) both indicated that the ibuprofen release was mainly controlled by diffusion.

The high shear wet granulation followed by the heat treatment and the drug loading procedure described in this work enabled pellets to be produced with physicochemical and textural properties close to the specifications concerning size, shape and porosity. Each step of the manufacturing procedure (granulation, heat treatment and loading procedure) was validated:

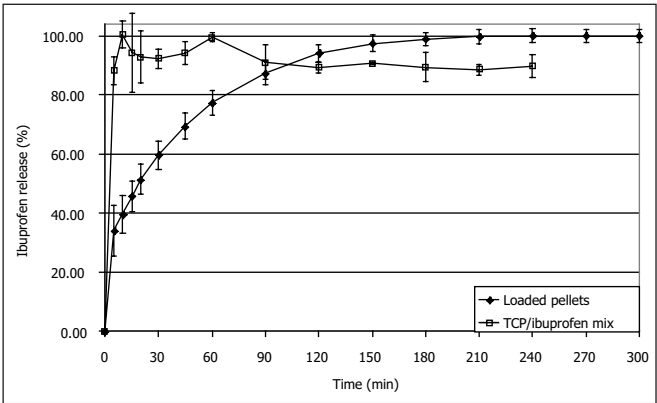


Figure 4 - Mean dissolution profile of ibuprofen from pellets (36 samples) versus CaP/ibuprofen mix.

Table VI - Modelled characteristics of the mean dissolution profile.

Models			Loaded pellets
Higuchi	$Q (\%) = at^{1/2} + b$	$r^2$	0.996
Hixson-Crowell	$\sqrt[3]{100 - \sqrt[3]{100 - Q}} = ct$	$r^2$	0.993
Ritger-Peppas	$Q (\%) = Kt^n$	$r^2$ $n$	0.986 0.33
Kopcha	$Q = A \sqrt{t} + Bt$	$r^2$ $A/B$	0.992 2.81

- physicochemical and textural properties of the four uncalcined pellet batches demonstrated the reproducibility of the granulation;
  - the similarity of their evolution after calcination validated the heat treatment;
  - the lack of statistical difference of intrabatch dissolution kinetics and drug contents established the reproducibility of the loading procedure.
- The same observation from batch to batch confirmed the previous conclusions concerning both the loading and the granulation steps.

Moreover, the process enabled pellets to be produced with the targeted ibuprofen quantity. These drug delivery systems entirely released the drug substance without *in vitro* disintegration, making them good candidates for *in vivo* implantation into bone defect cavities.

REFERENCES

1. LeGeros R.Z. - Calcium phosphate materials in restorative dentistry: a review. - *Adv. Dent. Res.*, **2**, 164-180, 1988.
2. Daculsi G., LeGeros R.Z., Nery E., Lynch K., Kerebel B. - Transformation of biphasic calcium phosphate ceramics *in vivo*: ultrastructural and physicochemical characterization. - *J. Biomed. Mat. Res.*, **23**, 883-894, 1989.
3. Passuti N., Daculsi G., Martin S., Basle M., Roher S. - Macroporous calcium phosphate ceramics for long bone surgery in human and dogs – Clinical and histological studies. - In: Heimke G., Soltesz U., Lee A.J.C. Eds., *Clinical Implants Materials. Advances in Biomaterials*, Elsevier Sciences Publishers, Amsterdam, 1990, pp. 255-258.
4. Daculsi G., LeGeros R.Z., Heughebaert M., Barbieux I. - Formation of carbonate-apatite crystals after implantation of calcium phosphate ceramics. - *Calcif. Tissue Int.*, **46**, 20-27, 1990.
5. LeGeros R.Z., Daculsi G., Orly I., Gregoire M., Heughebaert M., Gineste M., Kijkowska, R. - Formation of carbonate apatite on calcium phosphate materials: dissolution/precipitation processes. - In: Ducheyne, Kokubo and Van Blitterswijk Eds., *Bone-bonding*, Reed Healthcare Communications, 1992, pp. 201-212.
6. Vallet-Regi M., Gonzalez-Calbet J.M. - Calcium phosphates as



- substitution of bone tissues. - Progress in Solid State Chemistry, **32**, 1-31, 2004.
7. Hulbert S.F., Morrison S.J., Klawitter J.J. - Compatibility of porous ceramics with soft tissue; application to tracheal prostheses. - J. Biomed. Mater. Res., **5**, 269-279, 1971.
  8. Iveson S.M., Litster J.D., Hapgood K., Ennis B.J. - Nucleation, growth and breakage phenomena in agitated wet granulation processes: a review. - Powder Technol., **11**, 3-39, 2001.
  9. Plank R., Diehl B., Grinstead H., Zega J. - Quantifying liquid coverage and powder flux in high-shear granulators. - Powder Technol., **134**, 223-234, 2003.
  10. Corry D., Moran J. - Assessment of acrylic bone cement as a local delivery vehicle for the application of non-steroidal anti-inflammatory drugs. - Biomaterials, **19**, 1295-1301, 1998.
  11. Mendez J.A., Fernandez M., Gonzalez-Corchon M.A., Salvado M., Collia F., De Pedro J.A., Levenfeld B.L., Lopez-Bravo A., Vazquez B., San Roman J. - Injectable self-curing bioactive acrylic-glass composites charged with specific anti-inflammatory/analgesic agent. - Biomaterials, **25**, 2381-2392, 2004.
  12. Gonzalez-Corchon M.A., Salvado M., De la Torre B.J., Collia F., De Pedro J.A., Vazquez B., San Roman J. - Injectable and self-curing composites of acrylic/bioactive glass and drug systems. A histomorphometric analysis of the behaviour in rabbits. - Biomaterials, **27**, 1778-1787, 2006.
  13. Charnay C., Begu S., Tourne-Petel C., Nicole L., Lerner D.A., Devoiselle J.M. - Inclusion of ibuprofen in mesoporous templated silica: drug loading and release property. - Eur. J. Pharm. Biopharm., **57**, 533-540, 2004.
  14. Chevalier E., Viana M., Pouget C., Cazalbou S., Champion E., Chulia D. - From porous pellet fabrication to drug loading and release: the case of calcium phosphate matrix loaded with ibuprofen. - In: Bioceramics: Properties, Preparation and Applications, in press.
  15. Chevalier E., Viana M., Pouget C., Chulia D. - Influence of process parameters on pellets elaborated in a Mi-Pro high-shear granulator. - Pharm. Dev. Technol., **12**, 133-144, 2007.
  16. Viana M., Jouannin P., Pontier C., Chulia D. - About pycnometric density measurements. - Talanta, **57**, 583-593, 2002.
  17. Brunauer S., Emmett P.H., Teller E. - The use of low temperature Van der Waals adsorption isotherm in determining surface area. - J. Amer. Chem. Soc., **60**, 309-317, 1938.
  18. <http://rsb.info.nih.gov/ij/>
  19. Gabaude C.M., Gautier J.C., Saudemon P., Chulia D. - Validation of a new pertinent packing coefficient to estimate flow properties of pharmaceutical powders at a very early development stage, by comparison with mercury intrusion and classical flowability methods. - J. Mater. Sci., **36**, 1763-1773, 2001.
  20. Gibassier D., Sado P., Le Verge R., Devissaguet J.P. - Test de dissolution et fonction de Weibull. - Labo. Pharma. Prob. Techn., **30**, 250-255, 1982.
  21. Snedecor G.W., Cochran W.G. - Analysis of variance: the random effects model. - In: Statistical Methods, 8<sup>th</sup> ed., Iowa State University Press, Ames, Iowa, 1989, pp. 237-257.
  22. Knoop C., Vervier I., Thiry P., De Backer M., Kovarik J.M., Rousseau A., Marquet P., Estenne M. - Cyclosporine pharmacokinetics and dose monitoring after lung transplantation: comparison between cystic fibrosis and other conditions. - Transplantation, **4**, 683-688, 2003.
  23. Higuchi T. - Mechanism of sustained-action medication. Theoretical analysis of rate of release of solid drugs dispersed in solid matrices. - J. Pharm. Sci., **52**, 1145-1149, 1963.
  24. Hixson A.W., Crowell J.H. - Dependence of reaction velocity upon surface and agitation. - Ind. Eng. Chem., **23**, 923-931, 1931.
  25. Ritger P.L., Peppas N.A. - A simple equation for description of solute release. I. Fickian and non-Fickian release from non-swelling devices in the form of slabs, spheres, cylinders or discs. - J. Control. Rel., **5**, 23-36, 1987.
  26. Kopcha M., Lordi N., Tojo K.J. - Evaluation of release from selected thermosoftening vehicles. - J. Pharm. Pharmacol., **43**, 382-387, 1991.
  27. Pontier C. - Les phosphates de calcium apatitiques en compression. De la chimie aux qualités d'usage. - PhD Thesis, Université Paris-XI, Châtenay-Malabry, 2001, 243 p.
  28. Raynaud S., Champion E., Bernache-Assollant D. - Synthesis, sintering and mechanical characteristics of non stoichiometric apatite ceramics. - 11<sup>th</sup> Int Symposium on Ceramics in Medicine, New York, 1998, Bioceramics, **11**, pp. 109-112.
  29. Moore J.W., Flanner H.H. - Mathematical comparison of curves with an emphasis on *in vitro* dissolution profiles. - Pharm. Tech., **20**, 64-74, 1996.
  30. Shah V.P., Tsong Y., Sathe P. - *In vitro* dissolution profile comparison - statistics and analysis of the similarity factor, f<sub>2</sub>. - Pharm. Res., **15**, 889-896, 1998.

## ACKNOWLEDGMENTS

The authors thank the Région Limousin for its financial support. They are grateful to Eric Champion and Mickaël Palard for calcination and Miguel Viana for SEM observations. A special thank is addressed to Annick Rousseau for her help in statistical analyses.